

2015-01-22

Modelling the transfer of supraglacial meltwater to the bed of Leverett Glacier, Southwest Greenland

Clason, CC

<http://hdl.handle.net/10026.1/8100>

10.5194/tc-9-123-2015

The Cryosphere

All content in PEARL is protected by copyright law. Author manuscripts are made available in accordance with publisher policies. Please cite only the published version using the details provided on the item record or document. In the absence of an open licence (e.g. Creative Commons), permissions for further reuse of content should be sought from the publisher or author.



Modelling the transfer of supraglacial meltwater to the bed of Leverett Glacier, Southwest Greenland

C. C. Clason¹, D. W. F. Mair², P. W. Nienow³, I. D. Bartholomew³, A. Sole⁴, S. Palmer⁵, and W. Schwanghart⁶

¹Department of Physical Geography and Quaternary Geology, Stockholm University, 106 91 Stockholm, Sweden

²Geography and Environment, University of Aberdeen, Aberdeen, AB24 3UF, UK

³School of Geosciences, University of Edinburgh, Edinburgh, EH8 9XP, UK

⁴Department of Geography, University of Sheffield, Sheffield, S10 2TN, UK

⁵Geography, College of Life and Environmental Sciences, University of Exeter, Exeter, EX4 4RJ, UK

⁶Institute of Earth and Environmental Science, University of Potsdam, 14476 Potsdam-Golm, Germany

Correspondence to: C. C. Clason (caroline.clason@natgeo.su.se)

Received: 23 June 2014 – Published in The Cryosphere Discuss.: 29 July 2014

Revised: 12 December 2014 – Accepted: 24 December 2014 – Published: 22 January 2015

Abstract. Meltwater delivered to the bed of the Greenland Ice Sheet is a driver of variable ice-motion through changes in effective pressure and enhanced basal lubrication. Ice surface velocities have been shown to respond rapidly both to meltwater production at the surface and to drainage of supraglacial lakes, suggesting efficient transfer of meltwater from the supraglacial to subglacial hydrological systems. Although considerable effort is currently being directed towards improved modelling of the controlling surface and basal processes, modelling the temporal and spatial evolution of the transfer of melt to the bed has received less attention. Here we present the results of spatially distributed modelling for prediction of moulins and lake drainages on the Leverett Glacier in Southwest Greenland. The model is run for the 2009 and 2010 ablation seasons, and for future increased melt scenarios. The temporal pattern of modelled lake drainages are qualitatively comparable with those documented from analyses of repeat satellite imagery. The modelled timings and locations of delivery of meltwater to the bed also match well with observed temporal and spatial patterns of ice surface speed-ups. This is particularly true for the lower catchment (< 1000 m a.s.l.) where both the model and observations indicate that the development of moulins is the main mechanism for the transfer of surface meltwater to the bed. At higher elevations (e.g. 1250–1500 m a.s.l.) the development and drainage of supraglacial lakes becomes increasingly important. At these higher elevations, the delay between modelled melt generation and subsequent delivery of

melt to the bed matches the observed delay between the peak air temperatures and subsequent velocity speed-ups, while the instantaneous transfer of melt to the bed in a control simulation does not. Although both moulins and lake drainages are predicted to increase in number for future warmer climate scenarios, the lake drainages play an increasingly important role in both expanding the area over which melt accesses the bed and in enabling a greater proportion of surface melt to reach the bed.

1 Introduction

In the last decade it has been demonstrated that across large regions of the Greenland Ice Sheet (GrIS) surface meltwater is capable of penetrating through many hundreds of metres of cold ice via full-ice thickness crevasses, or moulins, and by the drainage of supraglacial lakes (e.g. Zwally et al., 2002; Das et al., 2008; Doyle et al., 2013). Evidence from remote sensing has shown the temporal and spatial patterns in lake formation and drainage during the melt seasons (e.g. McMillan et al., 2007; Sundal et al., 2009; Fitzpatrick et al., 2014) which indicates that the process is spatially extensive, with lake formation above 1800 m a.s.l. (Fitzpatrick et al., 2014). Once meltwater reaches the bed, the seasonal evolution of subglacial drainage system efficiency (e.g. Chandler et al., 2013), has been suggested to exert an important control on the dynamic response of the GrIS to surface melt-

water inputs due to its modulation of the relationship between surface meltwater inputs and subglacial water pressure (Bartholomew et al., 2010, 2011a; Colgan et al., 2011; Hoffman et al., 2011; Sole et al., 2013). Consequently there has been renewed interest and significant progress in developing spatially distributed, coupled models of subglacial hydrology and ice flow at the glacier and ice sheet scale (e.g. Hewitt, 2013; de Fleurian et al., 2014).

There has, however, been less attention focused on the development of models which can simulate the delivery of surface runoff to the bed of the ice sheet, i.e. modelling the temporal and spatial evolution of surface-to-bed meltwater connections (Clason et al., 2012; Banwell et al., 2013). This is a significant limitation since it is increasingly clear that the dynamics of the overlying ice may be most sensitive to hydrology when and where there are transient changes in meltwater delivery to the bed (Schoof, 2010; Bartholomew et al., 2012), and where ice thickness and surface slope precludes the formation of stable channelized drainage (Meierbachtol et al., 2013; Doyle et al., 2013). Aside from the overall contribution to dynamics through basal sliding, modelling of surface-to-bed meltwater connections may also be important for glacier dynamics through ice deformation, due to a potential influence on cryo-hydrologic warming (Phillips et al., 2010; Colgan et al., 2011). Models of delivery of supraglacial meltwater to the ice sheet bed are thus essential if physically based coupling of models of surface meltwater generation, subglacial hydrology and ice sheet dynamics is envisaged.

Here we apply a simple model which simulates spatial and temporal patterns in the delivery of meltwater to the bed of an ice sheet to one catchment of the Southwest GrIS. The model requires spatially distributed inputs of surface elevation, ice surface velocities, accumulation and air temperature. The model is run for the ablation seasons of 2009 and 2010 for which contemporaneous investigations of meteorology, hydrology and ice dynamics have been undertaken and reported elsewhere (Bartholomew et al., 2011a, b). We investigate the sensitivity of the model to parameters controlling refreezing, surface runoff delay and spatial resolution, and the effect of enhanced atmospheric warming on temporal and spatial patterns of modelled ice–bed meltwater connections. In the absence of detailed direct observations of supraglacial drainage system evolution, we assess qualitatively the performance of the model through (1) the consistency between modeled and observed patterns of supraglacial lake drainages, and (2) a comparison between timings and locations of modelled delivery of meltwater to the subglacial drainage system and the measured dynamic responses of the ice sheet to changing meltwater inputs.

2 Study area

Our study is focused on Leverett Glacier, a land-terminating outlet glacier of the Southwest GrIS, with its terminus sit-

uated at 67.1° N, 50.1° W. The supraglacial hydrological catchment upstream of the main proglacial river was derived from a digital elevation model (DEM) of the ice surface produced from Interferometric Synthetic Aperture Radar (InSAR) data acquired in 1996 (Palmer et al., 2011). The catchment encompasses an ice-covered area of c. 1200 km² and extends to over 50 km inland of the margin, up to an elevation of c. 1550 m (Fig. 1). Meltwater leaves the catchment through a large subglacial conduit (Fig. 1, yellow star), feeding a proglacial river. We focus our modelling on the 2009 and 2010 melt seasons when peak discharge in the proglacial river was 317 and 398 m³ s⁻¹, respectively (Bartholomew et al., 2011a).

3 Methods

The main components of the model, which has been applied in a previous version to the Croker Bay catchment of the Devon Ice Cap (Clason et al., 2012), comprise: (1) a degree-day model for meltwater generation; (2) an algorithm for routing meltwater across the ice surface (Schwanghart and Kuhn, 2010) and storing meltwater within supraglacial lakes; and (3) a model for calculating penetration depths of water-filled crevasses, after van der Veen (2007). The model, which is run here with a spatial resolution of 500 m and a temporal resolution of 1 day, is the first predictive (rather than prescriptive) model for moulin formation and the transfer of meltwater to the ice–bed interface applied to the Greenland ice sheet. Model outputs provide information on the location and timing of formation of surface-to-bed connections, the drainage of supraglacial lakes, the quantity of meltwater stored supraglacially and the quantity of meltwater delivered to the bed through each connection on each day.

3.1 Melt modelling and supraglacial meltwater retention

A lack of appropriate input data for energy balance modelling precludes its use here, so a degree-day model (Appendix A) was chosen for this application. Degree-day modelling is a simple approach for estimation of melting, but it has performed well in characterizing the relationship between melt and discharge in previous studies (Bartholomew et al., 2011b). Well calibrated degree-day factors (DDFs) for the catchment were calculated and calibrated for the Leverett glacier during 2009 (Appendix A). Meteorological data used for input to the degree-day model (Appendix A) were acquired at seven sites extending from the terminus of Leverett Glacier at 457 m (site 1, Fig. 1) into the ice sheet interior to 1716 m elevation (site 7, Fig. 1) (Bartholomew et al., 2011a). Daily accumulation was obtained from ultrasonic depth gauge measurements of surface height, and spring snowpack depth on 6 May 2009 was recorded at

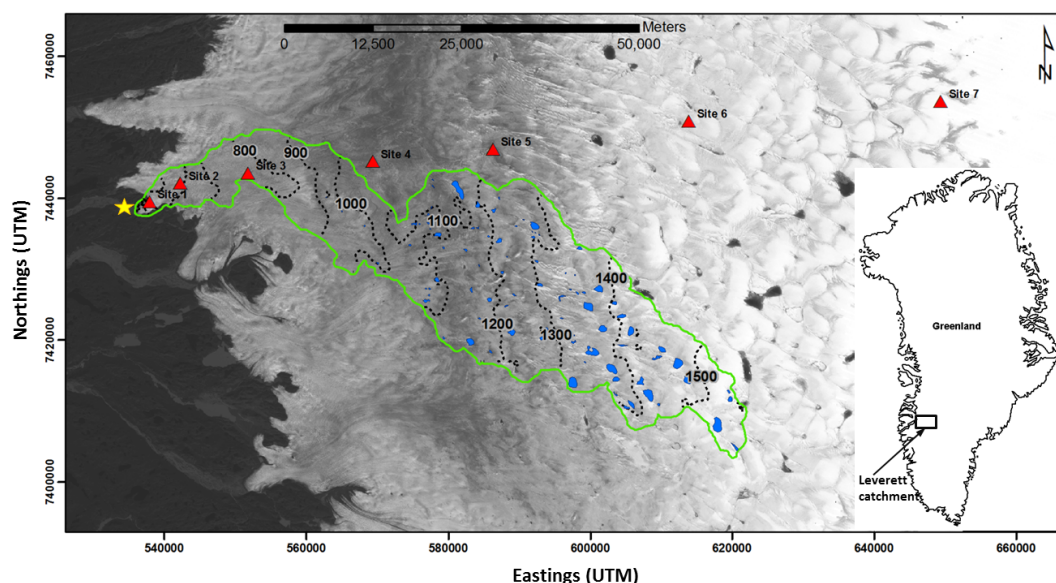


Figure 1. Leverett Glacier surface hydrological catchment (outlined in green). Contours show ice surface elevation (m a.s.l.); locations of meteorological data collection are depicted by red triangles; the location of proglacial discharge measurements is represented by the yellow star; and supraglacial lakes are highlighted in blue. The background image is from Landsat 7, band 2, captured on 5 August 2005.

each site (Fig. 1), resulting in an accumulation gradient of 256.6 mm w.e. per 1000 m ($R^2 = 0.76$).

Following application to the Croker Bay catchment (Clason et al., 2012) the model has been further developed to include both refreezing within the snowpack and a delay in meltwater routing across snow-covered cells. Model runs for the Leverett catchment without the inclusion of refreezing and runoff delay predicted lake drainages as early as May, which was not supported by observations, and studies such as Lefebvre et al. (2002) and Box et al. (2006) demonstrate the considerable effect of refreezing on runoff. After Reeh (1991), meltwater retention due to refreezing in the snowpack was included by implementing the simple P_{\max} coefficient, with a standard value of 0.6, supported by observations in the lower accumulation zone on west Greenland by Braithwaite et al. (1994). This coefficient is the fraction of the winter snowpack subject to refreezing over the course of a melt season, such that at the start of the model run P_{\max} is applied to the spring snowpack to determine refreezing potential in each cell. At each time step meltwater is refrozen instantaneously until the refreezing potential in each cell is met, whereby future melting is allowed to runoff. Following Schuler et al. (2007) we do not differentiate between pore-water refreezing and formation of superimposed ice.

To account for percolation and meltwater flow through the basal saturated layer a simple runoff delay, governed by local snow depth, was applied in all snow-covered cells. The length of the delay was based on flow rates for dye percolation through the snowpack and along the basal saturated layer of Haut Glacier d'Arolla (Campbell, 2007). The range of measured flow rates from Campbell (2007) give runoff de-

lays ranging from 1 to 16 days for meltwater flow through 1 m deep snow and along a 500 m flow path (model spatial resolution). In our model we incorporate a moderately high meltwater routing delay of 10 days for 1 m deep snow, scaling this delay linearly with local snow depth, and thus assuming a constant density summer snowpack, such that there is no delay when there is no snow.

3.2 Meltwater routing and accumulation in supraglacial lakes

A single-flow direction algorithm was applied to route available surface meltwater across the ice surface based on surface elevation (Schwanghart and Kuhn, 2010; Schwanghart and Scherler, 2014), where the amount of meltwater in each cell weighted downstream flow accumulation. The 100 m Palmer et al. (2011) DEM was resampled to the standard model spatial resolution of 500 m. We did not define a threshold for discrete stream formation due to the spatial resolution of the DEM; instead meltwater was distributed across the ice surface by flow accumulation only. A total of 93 supraglacial lakes within the Leverett catchment were manually digitized in ArcGIS from lake extents visible on Landsat 7 ETM+ imagery acquired on 15 and 31 July 2009 (Fig. 1), which were assumed to be maximum lake extents. A fixed number of empty lakes were thus prescribed at the start of the season, rather than expanding up-glacier as the area experiencing melting becomes larger.

Prescription of lakes based on digitization from satellite imagery was chosen instead of automated DEM-based identification of lakes (e.g. Leeson et al., 2012; Arnold et al.,

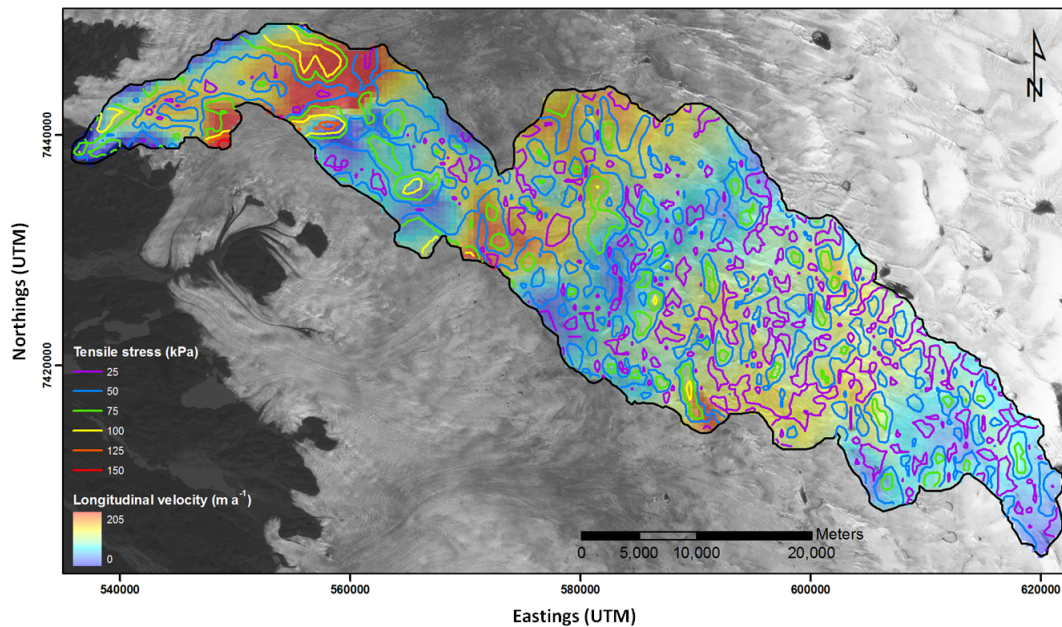


Figure 2. Longitudinally resolved (along-flow) ice surface velocities from InSAR data for the Leverett catchment (Joughin et al., 2010). Contours depict the ice surface tensile stress regime.

2014) to better capture the total number of lakes available for drainage. The 30 m resolution of Landsat imagery allows for higher accuracy than a 100 m resolution DEM in prescribing lake numbers and surface area, and furthermore, DEM-based models at best identify 78 % of lakes visible on remotely sensed imagery (Arnold et al., 2014). Modelled hydrofracture beneath lakes is very sensitive to meltwater volume, thus prescription of lakes from higher-resolution imagery was more appropriate for the purpose of predicting the timing of lake drainages and quantifying meltwater delivery to the bed. Given uncertainties associated with modelling lake volume based on depressions in DEMs, such as DEM vertical resolution, and since our model attempts only to predict when lakes drain, applying predictive tools to determine their location and maximum volume is beyond the requirements of this study.

Lake surface area was used to estimate lake volume based on a linear relationship derived between lake volume and surface area from data recorded by Box and Ski (2007) using MODIS for Southwest Greenland. There are two principal modes for supraglacial lake drainage: slow drainage events, where meltwater in lakes overtops and flows into downstream crevasses, moulins or other lakes (Hoffman et al., 2011; Tedesco et al., 2013); and fast drainage events, where large quantities of meltwater are delivered to the bed in a short period of time via hydrofracture, promoting a temporary ice dynamic response (e.g. Das et al., 2008; Doyle et al., 2013). Filling and overtopping of supraglacial lakes was accounted for within the flow accumulation routine (Clason et al., 2012) such that meltwater routed into a lake-

containing cell will accumulate until reaching the prescribed lake volume. At this point the lake will overtop and contribute to downstream runoff, which may flow into downstream crevasses if the lake has not already drained locally through modelled hydrofracture (Appendix C). Supraglacial lakes in Southwest Greenland are more numerous, have a larger total area, and have a larger frequency of fast drainage than anywhere else on the ice sheet (Selmes et al., 2011), making them an important feature of the Leverett glacier catchment.

3.3 Modelling crevasse location and depth

Synthetic aperture radar data from RADARSAT (Joughin et al., 2010) provided annual mean ice surface velocity data for the Leverett catchment from which velocity components (Fig. 2) and surface stresses could be calculated. The von Mises criterion, σ_v , after Vaughan (1993) was applied for calculation of tensile stresses, and crevasse locations were predicted based upon a prescribed tensile strength (Appendix B). The depth of each crevasse is calculated using a model of water-filled crevasse penetration based on linear elastic fracture mechanics (van der Veen, 2007) driven by accumulated surface meltwater and the surface tensile stress regime (Fig. 2; Appendix C). The volume flux of meltwater to the ice–bed interface is calculated at the bottom of each full ice thickness crevasse. In addition to the propagation of surface crevasses, fracture beneath supraglacial lakes, and their consequent drainage, is also permitted when lake meltwater volume is large enough to drive a fracture through the ice thickness at a specific location according to Eq. (C1)

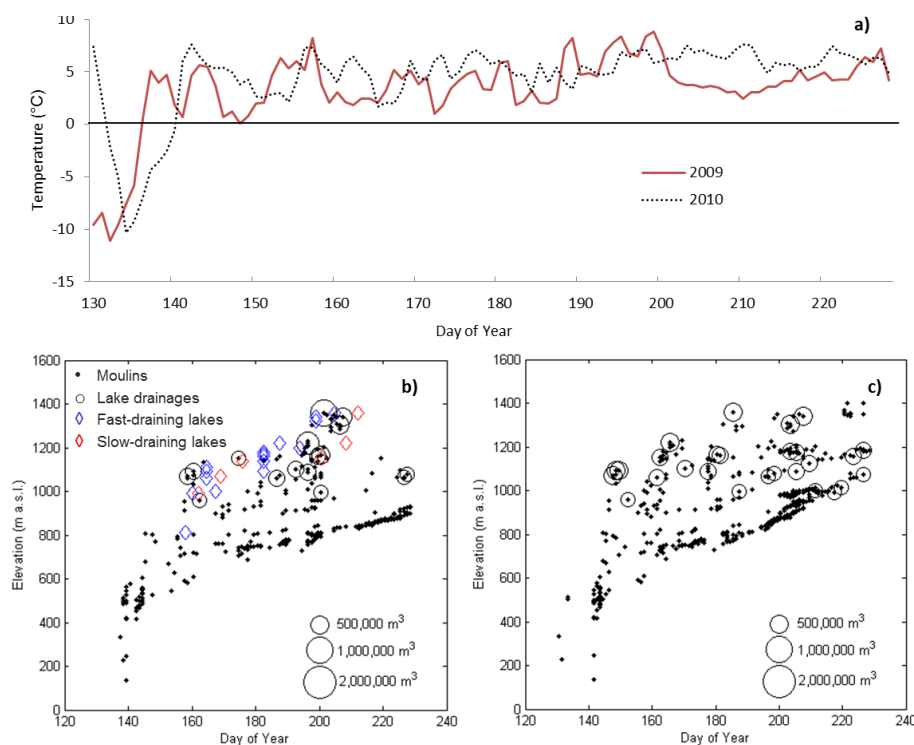


Figure 3. (a) Daily average air temperatures at site 1 (457 m a.s.l.) for 2009 and 2010, and moulin formation and lake drainage through the (b) 2009 and (c) 2010 melt seasons with elevation. Blue diamonds in (b) represent observed drainage of lakes in events between two MODIS images, and red diamonds represent lakes which drained over a period of several MODIS images; after Fig. 2a of Bartholomew et al. (2011a).

(Appendix C). Drainage of supraglacial lakes is permitted regardless of whether the tensile stress exceeds the prescribed ice tensile strength, since supraglacial lakes have been found to form in areas of low tensile or compressive surface stress (Catania et al., 2008).

4 Results

4.1 Application to Leverett 2009 and 2010 melt seasons

The model was first run for the 2009 melt season (run 1) with prescribed standard parameters of 75 kPa tensile strength, a 1 m depth-averaged crevasse width, an ice fracture toughness of $150 \text{ kPa m}^{1/2}$, P_{max} of 0.6, and a runoff delay of 10 days where snow is 1 m deep. In all subsequent runs these parameters remain the same unless otherwise stated. The timing of moulins first reaching the ice–bed interface in run 1 is depicted in Fig. 3b, where the number of moulins formed is shown to increase in elevation with time. This is due to expansion of the area experiencing melting, retreat of the snow-line, increased meltwater delay with elevation, and also due to the thicker ice through which moulins at higher elevation must penetrate to reach the bed. Supraglacial lake drainages also occur at higher elevations over time, as supported by remote sensing observations in Southwest Greenland (Morriss et al., 2013).

The model was also run using meteorological data from the 2010 melt season (run 2), covering the same time period as 2009 (day 130 to day 228), allowing for an assessment of model response to increased meltwater production in the Leverett catchment. During this period daily average temperatures at site 1 were on average 1°C higher than for 2009 (Fig. 3a). 2010 was characterized by high temperatures and significantly increased melt days across the GrIS, with temperatures highest in the west (Box et al., 2010). Melting occurred for up to 50 days longer than the 1979–2007 mean in areas of the western ice sheet, and during the month of May surface temperatures were as much as 5°C higher than the 1971–2000 average according to Reanalysis data from NCEP/NCAR. Figure 3c illustrates the modelled temporal formation of surface-to-bed connections during the 2010 melt season, where moulins begin forming one week earlier in comparison to the cooler 2009 season.

In 2009 modelled surface-to-bed connections form up to c. 1400 m (Fig. 4a), delivering 76 % of surface-generated meltwater to the bed. Below 1000 m elevation there are large clusters of moulins, which are cells for which sufficient meltwater is produced to allow for full-thickness fracture propagation of a single crevasse without relying on inflow from upstream accumulated meltwater. The model sets the runoff ratio, or the proportion of meltwater transferred to the next downstream cell, to zero when routed meltwater

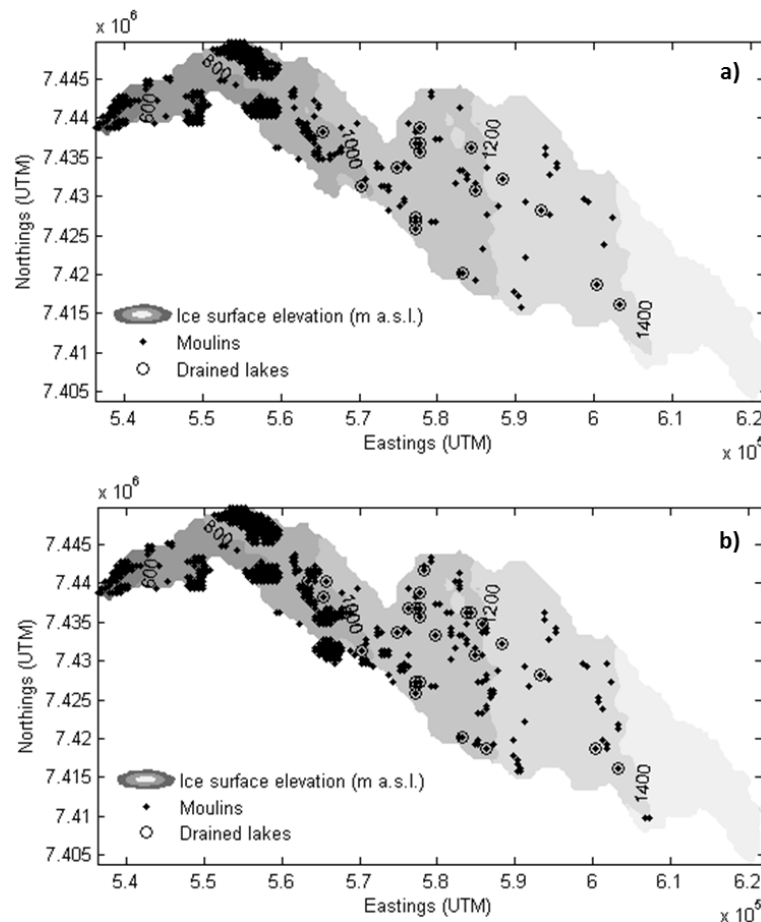


Figure 4. Spatial distribution of moulin and lake drainages for (a) 2009 and (b) 2010.

is captured by a crevasse. However, at low elevations melt rates are highest, enhanced by a smaller delay in meltwater transfer through cells with low spring snowpack depths. For the 2010 season the model predicts an increase in total moulin numbers of 44 % (Table 1) compared to 2009. Modelled lake drainages also increase in number from 17 in 2009 to 27 in 2010 (Table 1). Higher moulin numbers and lake drainages in 2010 causes the proportion of total meltwater that is (a) transferred to the bed to increase (by 9 %), and (b) stored supraglacially to decrease (by 5.7 %) (Table 1). In 2010 there is a notable increased clustering of moulins just below 1000 m and an increased number of lake drainages between 1100 and 1200 m elevation (Fig. 4b).

4.2 Sensitivity analysis

To investigate the influence of including refreezing within the model, P_{\max} was changed to 0.4 and 0 in runs 3 and 4. Moulin numbers showed a modest increase of 3.9 and 8.6 % for runs 3 and 4, respectively (Table 1). Associated increase in meltwater transfer to the bed of 4 and 10 % was balanced by a near identical 4.3 and 11 % decrease in supraglacial

meltwater storage, highlighting a strong control imposed by refreezing on meltwater availability for moulin formation.

The model was also tested for the upper and lower limits for runoff delay in runs 5 and 6, as derived from data by Campbell (2007). When a delay of only 1 day (at 1 m snow depth) was applied there was a small increase in moulin numbers of 5.2 %, due to the extended period during which melt is available to drive fracture propagation. Despite the increase in moulin numbers there was less than 1 % change in meltwater transfer to the bed and supraglacial storage (Table 1). Increasing the delay to 16 days for 1 m of snow had very little effect, with changes in meltwater transfer, storage and moulin numbers all less than 1 %. This is unsurprising as only the most upper reaches of the catchment are subject to the full meltwater transit delay, in an area receiving significantly less melt than in the lower elevation regions, where moulins are much less likely to form.

A limitation of the model is the control of spatial resolution on the number of crevasses with the potential to form connections to the bed. In runs 7 and 8 we thus ran the model at resolutions of 250 m and 1 km, respectively, excluding supraglacial lakes. Runs 7 and 8 produced a 50 %

Table 1. Total number of surface-to-bed connections formed, the percentage of surface-generated meltwater delivered to the bed and the percentage of surface-generated meltwater stored supraglacially via refreezing and percolation in the snowpack for each model run. Meltwater not accounted for by transfer to the bed or supraglacial storage is stored englacially inside crevasses which have not reached the bed.

Run name	Moulin numbers		Meltwater transfer		Supraglacial storage	
	Total moulins (number of lake drainages)	% change from initial run	% transfer from surface to bed	change from initial run	% of total generated meltwater	change from initial run
1 (2009)	327 (17)	n/a	76	n/a	17	n/a
2 (2010)	470 (27)	+44	85	+9.0	11	−5.7
3 ($P_{\max} = 0.4$)	340 (17)	+3.9	80	+4.0	13	−4.3
4 ($P_{\max} = 0$)	355 (17)	+8.6	86	+10	6.6	−11
5 (1-day runoff delay)	344 (16)	+5.2	77	+0.9	17	−0.5
6 16-day runoff delay)	329 (17)	+0.6	76	−0.2	17	+0.2
7 (250 m resolution)	489 (n/a)	+50	71	−5.1	17	0
8 (1 km resolution)	108 (n/a)	−67	81	+4.9	17	0
9 (A1B JJA min.)	479 (27)	+47	85	+8.8	12	−5.4
10 (A1B JJA mean)	549 (48)	+68	90	+14	8.0	−9.1
11 (A1B JJA max.)	685 (93)	+110	96	+20	3.7	−13

increase and 67 % decrease in moulin numbers respectively (Table 1), strongly controlled by the consequent changing number of surface crevasses. Although meltwater must be split between the available crevasses at each resolution, the available surface-produced meltwater is more than sufficient to drive many of these crevasses to the bed, resulting in only a small decrease in meltwater transfer of 5.1 % in run 7 and a small increase of 4.9 % in run 8. This relative insensitivity of meltwater transfer to changes in spatial resolution is encouraging for implementation within larger-scale ice sheet models. At such coarse spatial resolution prediction of the numbers of individual moulins is not yet possible, but prediction of areas where surface-to-bed meltwater transfer is an active process is important to simulate for subsequent forcing of subglacial hydrological models. There was no change in the amount of meltwater stored supraglacially in between runs 7 and 8 due to static controls on meltwater production and transport (Table 1). Instead, with an increase/decrease in crevasse numbers, the amount of water stored englacially in crevasses that do not reach the bed increases/decreases in runs 7 and 8, respectively. Since crevasse length is modified to equal cell width at each resolution, crevasse volume is also modified, resulting in a smaller quantity of meltwater necessary to produce the level of water-filling required to drive a crevasse to the bed.

Model sensitivity to tensile strength, fracture toughness and crevasse width was also tested for the Leverett domain, as described for application to the Croker Bay catchment on the Devon Ice Cap in Clason et al. (2012). Results of these tests illustrated the same model sensitivity to altering these parameters as was previously described: altering fracture toughness has no significant effect; altering tensile strength strongly influenced the total number of moulins due to controlling the number of surface crevasses; and while al-

tering crevasse width has no impact on crevasse numbers, it does influence the number of moulins through altering the volume of the crevasse and thus how much water is necessary to drive it to the bed. In summary these tests show that the most important control on the spatial extent of moulins is the value of the tensile strength. Parameters which define crevasse geometry affect the rate at which water will fill a crevasse and are most important in determining the timing of the delivery of surface meltwater to the bed.

4.3 Moulin and lake density

The spatial densities of modelled moulins and drained lakes in different elevation bands were calculated to investigate how the model characterizes the change in the mechanism for delivery of meltwater to the bed with elevation (Fig. 5). During the 2009 melt season, the model predicts a marked reduction in moulin density above 1000 m. Lake drainages only occur above 750 m elevation, with the highest density of drainages occurring between 1000 and 1250 m, incorporating site 4 (1061 m) and site 5 (1229 m) (Fig. 1), which exhibit the largest velocity peaks of the four sites above 1000 m.

4.4 Sensitivity to atmospheric warming

To investigate the sensitivity of ice surface-to-bed meltwater connections across the catchment to enhanced atmospheric warming, the model was run with the 2009 Leverett meteorological data revised to reflect the IPCC (2007) A1B scenario June, July and August air temperature projections for the Arctic region. 2009 was an average melt season based on the 1981–2010 mean (Sole et al., 2013), from which the three A1B scenarios (minimum, mean and maximum) represent temperature rises of 1.2, 2.1, and 5.3 °C, respectively (IPCC,

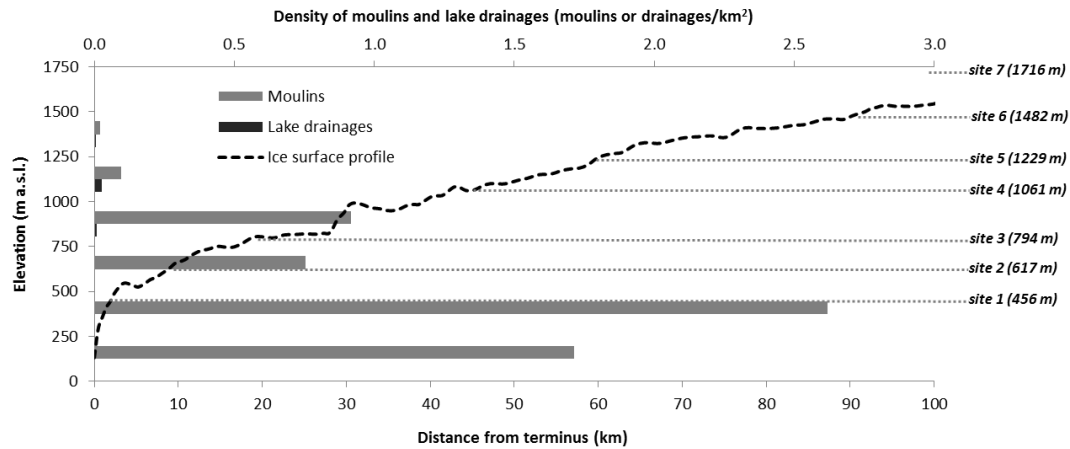


Figure 5. Density of moulins and lake drainages for 2009 within 250 m ice surface elevation bands. Sites of GPS velocity measurements (Fig. 1; Bartholomew et al., 2011b) are shown against the Leverett catchment ice surface profile. Note that only a very small area of the derived Leverett catchment lies below 500 m elevation, where outlet glaciers emerge at the margin of the ice sheet.

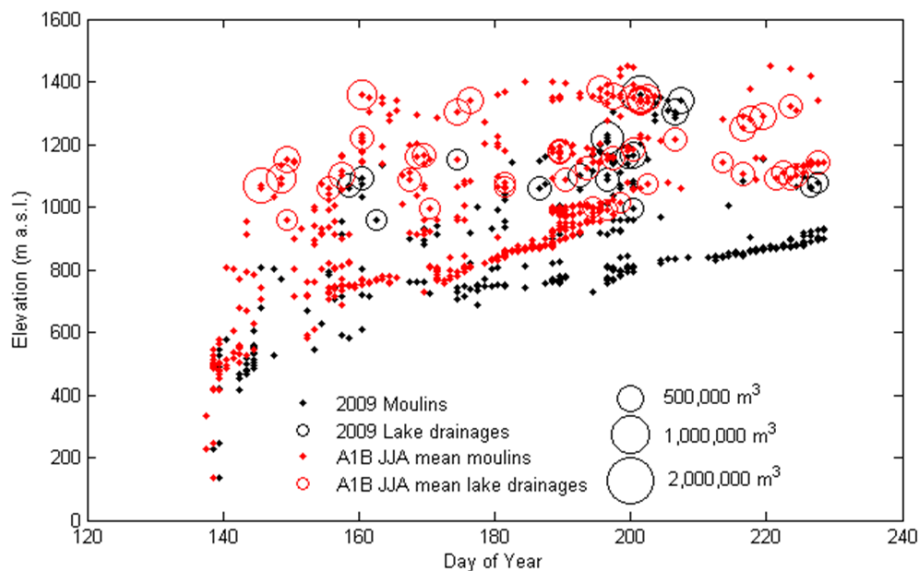


Figure 6. Spatial distribution of moulins and lake drainages for the 2009 melt season and the A1B mean June, July and August Arctic scenario of +2.1 °C (IPCC Fourth Assessment Report) applied to 2009 meteorological data.

2007), added uniformly to the 2009 temperature data. The results of running the model for increased future temperature scenarios (runs 9, 10 and 11; Table 1) show that in addition to an increase in moulin numbers (+47, 68 and 110 %) and much increased occurrence of lake drainages (+59, 182 and 447 %), applying these scenarios also resulted in increases of 8.8, 14 and 20 % in the proportion of surface-derived meltwater that is transferred to the bed, in comparison to model run 1.

Focusing on the mean scenario, below 750 m no change in moulin density is observed due to the smaller ice thicknesses and higher melt production resulting in all possible crevasses experiencing sufficient melt-filling to drive them

to the bed. Although the melt-season starts just a few days earlier, a temporal shift in moulin formation is evident, with moulins at higher elevation forming much earlier than for the standard 2009 model run (Fig. 6), and with an additional increase in the density of moulins at elevations above 750 m (Fig. 7). Furthermore, there is an increase in occurrence of lake drainages at higher elevations, resulting in more widespread delivery of meltwater to the bed through large ice thicknesses, beginning earlier in the melt season (Figs. 6 and 7).

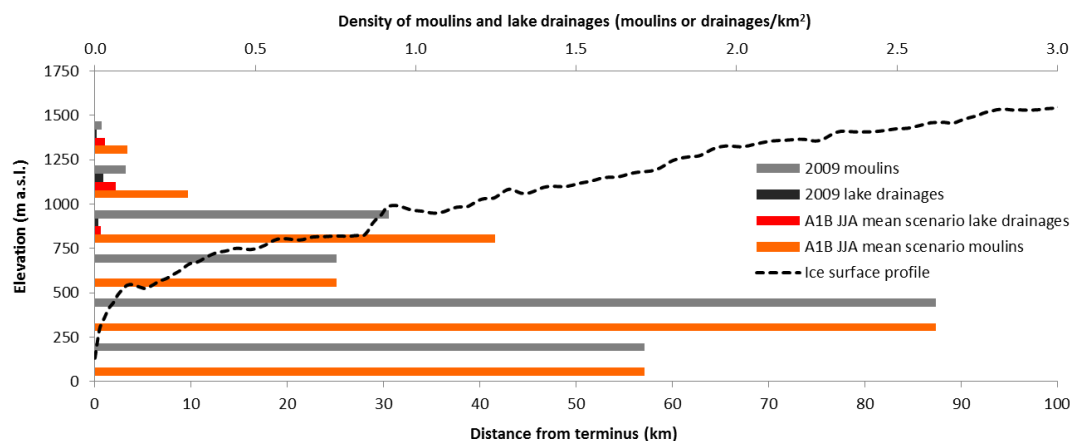


Figure 7. Density of moulins and lake drainages for A1B mean June, July and August Arctic scenario within 250 m ice surface elevation bands.

5 Assessment of model performance

5.1 Modelled and observed patterns of supraglacial lake drainage

A comparison between the modelled spatio-temporal pattern of lake drainages shown in Fig. 3a and a remote sensing-based assessment of lake drainage events in 2009 undertaken by Bartholomew et al. (2011a, their Fig. 2a) shows qualitative agreement. In both approaches: the majority of lakes drain between early June and mid-August; drainage of lakes mostly occurs between 1000 and 1400 m elevation, and there is a general trend showing an up-glacier progression in the timing of lake drainages of ~ 6 –8 m elevation per day. In comparison of Fig. 4a with Fig. 1 of Bartholomew et al. (2011a) there is spatial clustering of drained lakes between ~ 1000 and ~ 1200 m elevation in both cases. The model also predicts relatively isolated drainages of lakes approaching 1400 m, as observed by Bartholomew et al. (2011a) on MODIS imagery. Despite lake locations, surface areas, and thus maximum volumes being prescribed in this study, identified lakes are not preconditioned to drain through hydrofracture, and require sufficient meltwater input and ice surface stress to drain to the bed. While the model is not trying to reproduce exact observations of lake drainage, of the 17 lakes predicted to drain during 2009, 7 are contemporaneous with lake drainage locations identified by Bartholomew et al. (2011a); this is not unreasonable given the assumptions of the model and of determining lake locations and drainages from satellite imagery. These comparisons demonstrate that the model can reproduce realistic spatial and temporal patterns of lake drainage behaviour.

5.2 Modelled meltwater delivery to bed and measured dynamic responses during 2009

We further assess the performance of the model through the consistency between modelled patterns in the delivery of meltwater to the subglacial drainage system and measured dynamic response of the ice sheet to changing meltwater inputs for the 2009 melt season. During the 2009 melt season horizontal ice surface velocities were measured at seven GPS units, sites 1 to 7 (Fig. 1), extending from the Leverett glacier at 456 m up onto the ice sheet at 1716 m elevation (Bartholomew et al., 2011b). The period of the melt season characterized by highest velocities began later at sites of increasing elevation, with initial acceleration recorded at sites 1 and 2 shortly after the onset of melting, while increased velocities at sites 5 and 6 were not recorded until much later in the season. This is due to retreat of the snowline and onset of melting at increasingly high elevation. Furthermore, the periods of enhanced velocity at sites 4, 5 and 6 (all above 1061 m) are not strongly associated with high positive degree days at these sites, in contrast to sites 1, 2 and 3 (all below 800 m).

Meltwater transferred to the bed each day within each elevation band was calculated to compare the timing of modelled meltwater discharge to the bed with the timings of significant speed-up events within each elevation band (Fig. 8). Between 0 and 499 m elevation, there is relatively little meltwater delivered to the bed through moulins, which reflects the very small area of the Leverett catchment below 500 m. Periods of increasing meltwater delivery to the bed between 500 and 999 m match well with periods of velocity increase early in the season (Fig. 8c and d). At the highest elevations within the catchment, above 1250 m, between \sim day 200 and 210 there is also good agreement between the timing of meltwater delivery to the bed and the glacier speed-up. Between 1250 and 1499 m (Fig. 8), meltwater delivery to the bed is predicted in near-equal amounts from moulins and the

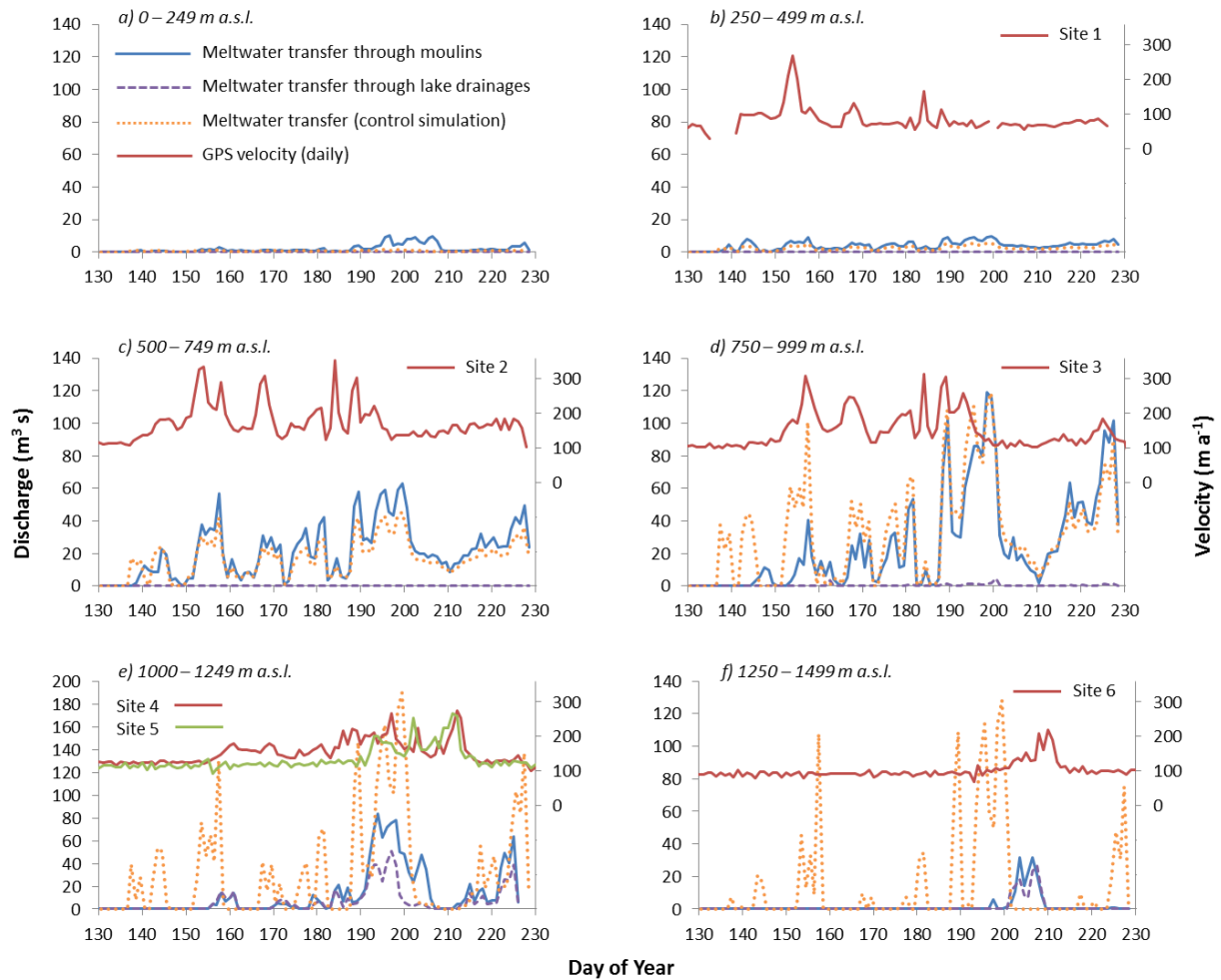


Figure 8. Supraglacial meltwater delivered to the bed each day through modelled lake drainages, moulins, and for the control simulation within ice surface elevation bands of 250 m during 2009. Ice surface velocities from GPS sites 1–6 are plotted within their respective elevation bands (after Bartholomew et al., 2011b). Note the extended y-axis in (e).

drainage of supraglacial lakes, highlighting the greater significance of lake drainages at high elevations.

To evaluate the necessity of predictive transfer of meltwater compared with routing all surface-generated meltwater to the bed (e.g. Shannon et al., 2013), a control simulation was run such that all meltwater was delivered to the bed locally and instantaneously, subject to storage and delay of meltwater through refreezing and percolation. The results of this control simulation (Fig. 8) reveal that without the additional modelling of surface meltwater runoff routing, hydrofracture through the ice, and the filling and drainage of supraglacial lakes, correspondence between the timing of increased meltwater transfer and increased ice surface velocities gets progressively worse with elevation. Between 750 and 999 m, meltwater transfer occurs early in the season, \sim day 135, with no corresponding velocity increase (Fig. 8d). At 1000–1249 m, the correspondence between velocity and meltwater transfer for the control simulation continues to worsen in the

early season, and breaks down completely for the whole season above 1250 m. These results highlight the importance of accounting for delay in meltwater transfer to the bed through storage in lakes, transport in supraglacial streams, and in meltwater delivery through moulins for which hydrofracture to the bed takes longer in areas of thicker ice.

6 Discussion

In light of future climate scenarios, incorporating the transfer of surface-derived meltwater to the bed is imperative if ice sheet models are to fully consider the behaviour and development of the subglacial drainage system, and the consequent ice velocity responses that drive ice sheet evolution and contribution to sea level change. This study has applied a model for prediction of moulin formation and lake drainages to data sets for the Leverett Glacier catchment in Southwest Greenland, simulating the delivery of meltwater from the ice

surface to the bed. The model was run for the 2009 and 2010 melt seasons and predicts high spatial densities of moulins below 1000 m as the principal mechanism for rapid delivery of meltwater to the glacier bed, a finding that is consistent with interpretations from field measurements of surface melting and velocity. Bartholomew et al. (2011b) suggested that at lower elevations, ice surface velocities respond to supraglacial meltwater routed quickly to the ice–bed interface through moulins, while at higher elevations the lack of correlation between positive degree days and ice velocities may be indicative of a dynamic response to the delayed release of meltwater stored in supraglacial lakes. Our model results are consistent with this finding, showing a similar change in the mechanism for the delivery of meltwater to the bed with elevation such that moulins are more dominant below 1000 m and drained lakes of more importance above this (Fig. 5). Above c. 1000 m lake drainages play a much greater role in ensuring that meltwater reaches the bed through propagation of crevasses up to 1100 m deep (see Doyle et al., 2013), and into the ice sheet interior.

Many previous studies have demonstrated that the most likely cause of short-term ice surface speed-ups is the creation of areas of high water pressure at the bed of the ice sheet in response to high meltwater inputs to a drainage system that is not hydraulically efficient enough to accommodate transient high discharges at low pressure (Hoffman et al., 2011; Bartholomew et al., 2012; Sole et al., 2013). Across most of the catchment there is a strong association between periods when the model predicts rapid increases in meltwater delivery to the bed and episodes of ice surface speed-up. The model output is therefore consistent with previous process interpretations. At GPS sites 1, 2 and 3 the period when the modelled meltwater discharges to the bed rise to a peak are not associated with speed-ups (\sim day 200). This is consistent with the proposition from interpretation of field evidence that in these regions of the ice sheet hydraulically efficient subglacial drainage channels eventually evolve which can accommodate high discharges at low pressures (e.g. Chandler et al., 2013).

The association between modelled meltwater delivery to the bed and observed ice sheet speed-ups is less obvious between 1000 and 1249 m a.s.l. (GPS sites 4 and 5). This may reflect model inadequacies or the effects of presenting modelled discharge as integrated values across an elevation band that covers a large horizontal extent. This elevation band is also likely to encompass the up-glacier limit in the extent to which efficient subglacial channels can evolve. Chandler et al. (2013) argued that channelized drainage could evolve up to 41 km from the ice sheet margin where the ice surface lies at a little over 1000 m a.s.l., i.e. at the lower range of this elevation band. However, this study also showed that inferred channels did not extend as far as 57 km where the ice sheet surface was 1230 m a.s.l. which is close to the upper range of the elevation band. Modelling of subglacial conduits by Meierbachtol et al. (2013) places an even lower limit

of \sim 20 km on the up-ice extent of subglacial conduits, arguing that low surface slopes up-ice of the margin inhibit melting back of conduit walls. The conduits therefore cannot offset creep closure to accommodate increasing discharge. It is therefore likely that in the 1000–1249 m a.s.l. elevation band there is considerable spatial heterogeneity in subglacial drainage system evolution which would reduce the likelihood of observing a clear temporal association between spatially integrated modelled discharge and ice surface velocity. This assumption is supported by recent observations of hydraulic head and ice surface velocity in west Greenland by Andrews et al. (2014).

At the highest elevations within the catchment several processes combine to delay the delivery of meltwater to the bed: the vertical percolation and refreezing of melt in the snowpack, the slowing of horizontal surface runoff through the snowpack, and the accumulation of sufficient water in supraglacial lakes to initiate full-depth crevasse formation. The close agreement between the timing of modelled meltwater delivery to the bed and surface velocity speed-ups at the highest elevations in the catchment indicate that the model is able to characterize these processes effectively. This meltwater is delivered to the bed several days after the peak atmospheric temperatures during a relatively cool period between days 200 and 210 (see Figs. 3a and 8).

The comparison between 2009 and the warmer 2010 melt season and the testing of the sensitivity of the model results to atmospheric warming provides insight into how the catchment's hydrology may change under a warmer climate. The model shows the potential for an increased proportion of supraglacial meltwater to reach the bed, and that a larger area of the bed is directly affected by surface meltwater inputs, owing to the up-glacier expansion in the area affected by supraglacial lake drainages. This latter model outcome is supported by observations of an expansion in lake-covered area during warm years in the Russell Glacier catchment (Fitzpatrick et al., 2014). The modeled quantities of meltwater accessing the bed through lake drainage events shown here under the warmer climate scenarios are likely to give us a conservative view of what might be expected across the GrIS more generally, for two reasons. Firstly, the model uses a fixed, prescribed pattern of supraglacial lake cells which does not expand higher up-glacier as the melt extent increases. Secondly, the Leverett catchment only extends to c. 1550 m elevation and so cannot characterize the potential for a vast increase in the area where supraglacial lakes could form under a warmer climate. Both of these issues could be addressed by coupling this model with one that can predict the location of the formation of supraglacial lakes (e.g. Leeson et al., 2012). Nevertheless, the model clearly indicates that under a moderately warmer climate there will be an increase in the relative importance of supraglacial lake drainage in delivering melt to the bed of the ice sheet in the high-elevation areas of the ice sheet (above 1000 m elevation) despite ice thicknesses in excess of 1 km.

It is not clear what the long-term impact of more spatially extensive and more frequent lake drainages may be on longer-term ice dynamics across high-elevation areas of the ice sheet. Across the ablation area of the ice sheet it has been shown that there is no significant correlation between normalized surface melt and annual ice flow (Sole et al., 2013). It has been proposed that increased summer melting sustains large, widespread low-pressure subglacial channels which in turn promote more extensive and prolonged drainage of high pressure water from adjacent regions resulting in a greater drop in net basal water pressure and reduced displacement over the subsequent winter (Sole et al., 2013; Tedstone et al., 2013). This preconditioning of the ice–bed interface for reduced winter velocity limits the ice sheet’s dynamic sensitivity to interannual variations in surface temperature and melt. However, a positive relationship between warmer summer air temperatures and annual velocities may be expected well above the ELA where the development of low-pressure channelized drainage is likely hindered by greater ice thicknesses and shallow surface slopes (Meierbachtol et al., 2013; Doyle et al., 2013). The long-term implications of increased melting during warmer years, such as that witnessed in 2010 and 2012 (Tedstone et al., 2013), on subglacial drainage configuration, basal water pressure, and consequently ice dynamics, are difficult to assess without coupling a model such as the one presented here to subglacial drainage and ice flow models (e.g. Hewitt, 2013; de Fleurian et al., 2014; Hoffman and Price, 2014).

7 Conclusions

A spatially distributed model for predicting the temporal and spatial patterns of moulin formation and lake drainages has been applied to the Leverett Glacier in Southwest Greenland. With minimal data requirements and a simple structure, the model is easily transferable to other areas, including those without supraglacial lakes. The model was run for the 2009 and 2010 ablation seasons, driven by in situ meteorological and melt observations, and assessed by comparison with independent interpretations of meltwater delivery to the bed based on analyses of ice dynamic response to atmospheric forcings. The response of the catchment’s hydrology to future climate scenarios is also investigated, as is the model sensitivity to parametrization of refreezing, horizontal meltwater transit through surface snowpacks and the model’s spatial resolution.

The model is successful in characterizing the spatial variation in the mechanisms for meltwater transfer from the surface to the bed. For the lower part of the catchment (< 1000 m a.s.l.) both the model and previous observations indicate that the development of moulins is the main mechanism for the transfer of surface meltwater to the bed. At the highest elevations (e.g. 1250–1500 m a.s.l.) the development and drainage of supraglacial lakes becomes increasingly important.

At the higher elevations, the delay between modelled melt generation and subsequent delivery of melt to the bed matches the observed delay between the peak air temperatures and subsequent velocity speed-ups. This indicates that the model effectively characterizes processes which delay the delivery of surface-generated melt to the ice sheet bed.

The temporal and spatial patterns of modelled lake drainages compare favourably with those seen from analyses of satellite imagery. The modelled timings and locations of delivery of meltwater to the bed match well with observed temporal and spatial patterns of ice surface speed-ups.

Results of modelling moulin formation and lake drainage for the warmer 2010 season, and particularly for future climate scenarios, indicate the potential for increased absolute and relative transfer of supraglacial meltwater to the bed during periods of increased surface melting. With atmospheric warming lake drainages play an increasingly important role in both expanding the area over which surface-derived melt accesses the bed and in enabling a greater proportion of surface melt to reach the bed. Model sensitivity testing demonstrates that the proportion of melt reaching the bed is relatively insensitive to refreezing thresholds, runoff delays and the spatial resolution of the model.

This work contributes to efforts to couple physically based models of surface meltwater generation, subglacial hydrology and ice sheet dynamics which will be required to fully understand past, contemporary and future sensitivity of ice sheet mass balance and dynamics to climate change.

Appendix A: Degree-day modelling

The model runs at a daily time step, and values of total melting each day, M_t , are determined by the application of a degree-day factor (DDF) for every day where mean temperature, T_t , equals or exceeds 0°C :

$$M_t = (\text{DDF} \cdot T_t) \quad T_t \geq 0^\circ\text{C} \quad (\text{A1})$$

$$M_t = 0 \quad T_t < 0^\circ\text{C}. \quad (\text{A2})$$

The sum of daily melt values occurring over N days thus gives total ablation, A :

$$A = \sum_{i=1}^N M_t. \quad (\text{A3})$$

A DDF for snow (DDF_s) is applied for snow-covered cells, with a DDF for ice (DDF_i) applied when the cumulative melt exceeds the prescribed spring snowpack depth. Precipitation falling as snow is added to the snowpack depth, but rainfall, where air temperature is above 1°C , is not included within the melt model due to the very small contribution it makes to total melt.

Temperature was recorded at 15 min intervals at each of seven sites in the Leverett catchment (Fig. 1) during the 2009 and 2010 melt seasons. The model is run for the contemporaneous period of data collection from 10 May (day 130) to 16 August (day 228) for each year. An air temperature lapse rate of 5.5°C per 1000 m was calculated from the 2009 data ($R^2 = 0.96$). Degree-day factors for snow and ice (DDF_s and DDF_i) of 5.81 and 7.79 mm w.e. $\text{d}^{-1}^\circ\text{C}^{-1}$, respectively, were determined based on calibration against ablation rates recorded by ultrasonic depth gauges during 2009.

Appendix B: Identification of areas of surface crevassing

Velocity data were first resolved into longitudinal and transverse components (Fig. 2), the directional derivatives of which were then used to calculate strain rates, $\dot{\epsilon}_{ij}$. After Nye (1957), the constitutive relation was applied to convert strain rates to stresses, σ_{ij} :

$$\sigma_{ij} = B \dot{\epsilon}_e^{(1-n)/n} \dot{\epsilon}_{ij}, \quad (\text{B1})$$

where $\dot{\epsilon}_e$ is effective strain, and n is the flow law exponent with a value of 3. B is a viscosity parameter sensitive to ice temperature, and is related to the flow law as $B = A^{-1/n}$ (Vieli et al., 2006). For the Leverett catchment we apply an ice temperature of -5°C , giving a flow law parameter, A , value of $9.3 \times 10^{-16} \text{ s}^{-1} \text{ kPa}^{-3}$ (Cuffey and Paterson, 2010) and a viscosity parameter, B , value of $324 \text{ kPa a}^{1/3}$.

For determining areas containing surface crevassing, ice surface tensile stresses, R_{ij} , were calculated based on the von Mises criterion, σ_v , after Vaughan (1993):

$$\sigma_v = (\sigma_1 \sigma_1) + (\sigma_3 \sigma_3) - (\sigma_1 \sigma_3), \quad (\text{B2})$$

where the maximum and minimum principal stresses, σ_1 and σ_3 , are calculated from

$$\sigma_1 = \sigma_{\max} = \frac{1}{2} (\sigma_{xx} + \sigma_{yy}) + \sqrt{\left[\frac{1}{2} (\sigma_{xx} - \sigma_{yy}) \right]^2 + \tau_{xy}^2} \quad (\text{B3})$$

$$\sigma_3 = \sigma_{\min} = \frac{1}{2} (\sigma_{xx} + \sigma_{yy}) - \sqrt{\left[\frac{1}{2} (\sigma_{xx} - \sigma_{yy}) \right]^2 + \tau_{xy}^2} \quad (\text{B4})$$

and where σ_{xx} , σ_{yy} and τ_{xy} are the longitudinal, transverse and shear stresses respectively. The tensile stress is thus related to the von Mises criterion as

$$R_{ij} = \sqrt{\sigma_v}. \quad (\text{B5})$$

Model cells containing surface crevassing were determined by prescribing a value of tensile strength, based on visual matching of the calculated surface tensile stresses (Fig. 2) with crevassing visible on Landsat 7 imagery. A tensile strength of 75 kPa was thus prescribed in the standard model parameters. This was the value that best represented spatial distribution of crevassing on imagery, without over-prediction of crevasses in higher-elevation areas with numerous supraglacial lakes, which would have acted to impede lake filling through meltwater routing. This visual comparison approach was very simple, and based on tensile stresses calculated from annual mean velocities. For future applications we would recommend deriving tensile stresses from summer velocities where data exist, to ensure prescribing the most representative tensile strength for the ablation season. The tensile stresses are used both as an input to crevasse depth modelling and also for determining the runoff ratio of meltwater routed across the ice surface. The runoff ratio is 1 where cells do not contain crevasses, and 0 when tensile stresses exceed the prescribed tensile strength, such that upstream runoff is captured by surface crevasses, resetting downstream flow accumulation to zero.

Appendix C: Calculation of crevasse depths

The model uses accumulated surface meltwater and the surface tensile stress regime (Fig. 2) as inputs to a model of water-filled crevasse penetration to calculate crevasse depth, d , based on linear elastic fracture mechanics, after van der Veen (2007):

$$K_I = 1.12 R_{xx} \sqrt{\pi d} - 0.683 \rho_i g d^{1.5} + 0.683 \rho_w g b^{1.5}. \quad (\text{C1})$$

The net stress intensity factor, K_I , which describes elastic stresses incident on the tip of a crevasse, is found by summing the terms on the right which describe stress intensity

factors relating to the tensile stress, the lithostatic stress of the ice, and the effect of water-filling within the crevasse. Acceleration due to gravity g , density of ice ρ_i and density of freshwater ρ_w are assigned the standard values of 9.81 m s^{-2} , 918 and 1000 kg m^{-3} respectively. Surface tensile stresses R_{xx} derived from velocity data are used as input to the first term in the right-hand side. Meltwater accumulated in each cell determines the water level in a crevasse, b , in the third term using Q , the rate at which a crevasse is filled with water, and time, t , where

$$b = Qt. \quad (\text{C2})$$

The level of the meltwater, b , in a crevasse is also controlled by crevasse geometry. Accumulated daily surface meltwater is calculated as a depth of water equivalent generated across each $500 \text{ m} \times 500 \text{ m}$ cell. This water then converges into the prescribed surface area of a crevasse when applied to Eq. (C1). The model assumes one crevasse per cell, and crevasse surface dimensions are prescribed as a depth-averaged width of 1 m and a length of 500 m (cell width) for the standard model runs. The width was prescribed at 1 m to represent a depth-average of observed crevasse widths in Greenland, ranging from the scale of metres at depth below the ice surface (e.g. Cook, 1956), to centimetres or decimetres as crevasses narrow towards the surface (e.g. Doyle et al., 2013).

The fracture toughness of ice, K_{IC} , is the critical stress at which a pre-existing flaw will begin to propagate, for which we prescribe a fracture toughness of $150 \text{ kPa m}^{1/2}$ as an average of values calculated by Fischer et al. (1995) and Rist et al. (1999). We prescribe an initial crevasse depth, or pre-existing flaw, of $1 \times 10^{-7} \text{ m}$ to ensure initiation of fracture propagation. Solving iteratively for depth, d , until K_I is less than the prescribed ice fracture toughness, K_{IC} , the model calculates the propagation depth of each crevasse. Crevasse propagation depths are calculated each day for cells where R_{xx} equals or exceeds the prescribed tensile strength, with depth increasing with time while propagation continues in response to daily accumulated surface meltwater.

The locations of moulins, delivering meltwater to the ice–bed interface, are predicted when crevasse depth equals ice thickness, which is based upon a 5 km ice thickness data set derived from ice-penetrating radar (Bamber et al., 2001). In this study we imply that a moulin is any connection where surface meltwater has forced propagation of a crevasse through the full ice thickness between the ice surface and the ice–bed interface, including crevasses beneath drained lakes. Intersection of supraglacial streams and surface crevasses can initiate the formation of traditional, circular moulins, although many of these connections will close within 1 year due to refreezing and due to creep closure of crevasses when the supply of meltwater is shut off (van der Veen, 2007). It is thus not assumed that the modelled surface-to-bed connections must take the form of traditional moulins, nor does the model account for perennial moulins reopened after the accumulation season.

The drainage of supraglacial lakes, identified by manual digitization of Landsat imagery, is accounted for within the model where it is assumed that a crevasse is present beneath each lake, regardless of the local tensile stress. The volume of meltwater stored in each lake is used to calculate the depth of meltwater within a crevasse, b , at each daily time step, converting stored meltwater in mm w.e. to crevasse water depth in m w.e. , and adjusted for crevasse width and length. Drainage of lakes within one 24 h time step is supported by the sub-daily drainage of supraglacial lakes witnessed in Southwest Greenland by Das et al. (2008) and Doyle et al. (2013). Thus when Eq. (9) is solved for $K_I \geq K_{IC}$, where d is set to equal the ice thickness, lakes drain to the bed within one model time step since lake meltwater content has reached a level sufficient for crevasse propagation through the full ice thickness.

Author contributions. The modelling approach was developed by C. C. Clason, with meteorological and velocity data for Leverett glacier contributed by A. Sole and I. D. Bartholomew. The experimental concept was developed by C. C. Clason, D. W. F. Mair and P. W. Nienow. S. Palmer contributed the ice surface DEM, and W. Schwanghart developed the flow accumulation and lake filling subroutine. C. C. Clason wrote the original draft with contribution from D. W. F. Mair.

Acknowledgements. We acknowledge the College of Physical Sciences, University of Aberdeen, the Leverhulme Trust through a Study Abroad Studentship and the Swedish Radiation Safety Authority, for funding awarded to C. Clason. Data collection was supported by the UK Natural Environment Research Council (through a studentship to I. Bartholomew and grants to P. Nienow and D. Mair) and the Edinburgh University Moss Centenary Scholarship (I. Bartholomew). We acknowledge I. Joughin for providing InSAR velocity data, and the National Snow and Ice Data Centre, University of Colorado, and J. Bamber for ice thickness data. We thank two anonymous reviewers for their comments which helped to improve the paper.

Edited by: G. H. Gudmundsson

References

- Andrews, L. C., Catania, G. A., Hoffman, M. J., Gulley, J. D., Lüthi, M. P., Ryserm C., Hawley, R. L., and Neumann, T. A.: Direct observations of evolving subglacial drainage beneath the Greenland Ice Sheet, *Nature*, 514, 80–83, doi:10.1038/nature13796, 2014.
- Arnold, N. S., Banwell, A. F., and Willis, I. C.: High-resolution modelling of the seasonal evolution of surface water storage on the Greenland Ice Sheet, *The Cryosphere*, 8, 1149–1160, doi:10.5194/tc-8-1149-2014, 2014.
- Bamber, J. L., Layberry, R. L., and Gogineni, S. P.: A new ice thickness and bed data set for the Greenland ice sheet: 1. Measurement, data reduction, and errors, *J. Geophys. Res.*, 106, 33773–33780, 2001.
- Banwell, A. F., Willis, I. C., and Arnold, N. S.: Modeling subglacial water routing at Paakitsoq, W Greenland, *J. Geophys. Res.-Earth*, 118, 1282–1295, 2013.
- Bartholomew, I., Nienow, P., Mair, D., Hubbard, A., King, M., and Sole, A.: Seasonal evolution of subglacial drainage and acceleration in a Greenland outlet glacier, *Nat. Geosci.*, 3, 408–411, 2010.
- Bartholomew, I., Nienow, P., Sole, A., Mair, D., Cowton, T., Palmer, S., and Wadham, J.: Supraglacial forcing of subglacial drainage in the ablation zone of the Greenland ice sheet, *Geophys. Res. Lett.*, 85, L08502, doi:10.1029/2011GL047063, 2011a.
- Bartholomew, I. D., Nienow, P., Sole, A., Mair, D., Cowton, T., King, M. A., and Palmer, S.: Seasonal variations in Greenland Ice Sheet motion: Inland extent and behaviour at higher elevations, *Earth Planet. Sc. Lett.*, 307, 271–278, 2011b.
- Bartholomew, I., Nienow, P., Sole, A., Mair, D., Cowton, T., and King, M. A.: Short-term variability in Greenland Ice Sheet motion forced by time-varying meltwater drainage: Implications for the relationship between subglacial drainage system behaviour and ice velocity, *J. Geophys. Res.*, 117, F03002, doi:10.1029/2011JF002220, 2012.
- Box, J. E. and Ski, K.: Remote sounding of Greenland supraglacial melt lakes: implications for subglacial hydraulics, *J. Glaciol.*, 53, 257–265, 2007.
- Box, J. E., Bromwich, D., Veenhuis, B., Bai, L. S., Stroeve, J., Rogers, J., Steffen, K., Haran, T., and Wang, S. H.: Greenland Ice Sheet Surface Mass Balance Variability (1988–2004) from Calibrated Polar MM5 Output, *J. Climate*, 19, 2783–2800, 2006.
- Box, J. E., Cappelen, J., Decker, D., Fettweis, X., Mote, T., Tedesco, M., and van de Wal, R. S. W.: Greenland, Arctic Report Card 2010, <http://www.arctic.noaa.gov/reportcard> (last access: 17 June 2014), 2010.
- Braithwaite, R. J., Laternser, M., and Pfeffer, W. T.: Variations of near-surface firn density in the lower accumulation area of the Greenland ice sheet, Pakitsoq, West Greenland, *J. Glaciol.*, 40, 477–485, 1994.
- Campbell, F. M. A.: The role of supraglacial snowpack hydrology in mediating meltwater delivery to glacier systems, PhD thesis, University of Glasgow, Glasgow, UK, 227 pp., <http://theses.gla.ac.uk/2871/> (last access: 17 June 2014), 2007.
- Catania, G. A., Neumann, T. A., and Price, S. F.: Characterizing englacial drainage in the ablation zone of the Greenland ice sheet, *J. Glaciol.*, 54, 567–578, 2008.
- Chandler, D. M., Wadham, J. L., Lis, G. P., Cowton, T., Sole, A., Bartholomew, I., Telling, J., Nienow, P., Bagshaw, E. B., Mair, D., Vinen, S., and Hubbard, A.: Evolution of the subglacial drainage system beneath the Greenland Ice Sheet revealed by tracers, *Nat. Geosci.*, 6, 195–198, 2013.
- Clason, C. C., Mair, D. W. F., Burgess, D. O., and Nienow, P. W.: Modelling the delivery of supraglacial meltwater to the ice/bed interface: application to the southwest Devon Ice Cap, Nunavut, Canada, *J. Glaciol.*, 58, 361–374, 2012.
- Colgan, W., Steffen, K., McLamb, W. S., Abdalati, W., Rajaram, H., Motyka, R., Phillips, T., and Anderson, R.: An increase in crevasse extent, West Greenland: Hydrologic implications, *Geophys. Res. Lett.*, 38, L18502, doi:10.1029/2011GL048491, 2011.
- Cook, J. C.: Some Observations in a Northwest Greenland Crevasse, *Transactions, Am. Geophys. Union*, 37, 715–718, 1956.
- Cuffey, K. M. and Paterson, W. S. B.: *The Physics of Glaciers*, 4th Edn., Butterworth-Heinemann, Oxford, 2010.
- Das, S. B., Joughin, I., Behn, M. D., Howat, I. M., King, M. A., Lizarralde, D., and Bhatia, M. P.: Fracture Propagation to the Base of the Greenland Ice Sheet During Supraglacial Lake Drainage, *Science*, 320, 778–781, 2008.
- de Fleurian, B., Gagliardini, O., Zwinger, T., Durand, G., Le Meur, E., Mair, D., and Råback, P.: A double continuum hydrological model for glacier applications, *The Cryosphere*, 8, 137–153, doi:10.5194/tc-8-137-2014, 2014.
- Doyle, S. H., Hubbard, A. L., Dow, C. F., Jones, G. A., Fitzpatrick, A., Gusmeroli, A., Kulesa, B., Lindback, K., Pettersson, R., and Box, J. E.: Ice tectonic deformation during the rapid in situ drainage of a supraglacial lake on the Greenland Ice Sheet, *The Cryosphere*, 7, 129–140, doi:10.5194/tc-7-129-2013, 2013.
- Fischer, M. P., Alley, R. B., and Engelder, T.: Fracture toughness of ice and firn determined from the modified ring test, *J. Glaciol.*, 41, 383–394, 1995.
- Fitzpatrick, A. A. W., Hubbard, A. L., Box, J. E., Quincey, D. J., van As, D., Mikkelsen, A. P. B., Doyle, S. H., Dow, C. F., Hasholt,

- B., and Jones, G. A.: A decade (2002–2012) of supraglacial lake volume estimates across Russell Glacier, West Greenland, *The Cryosphere*, 8, 107–121, doi:10.5194/tc-8-107-2014, 2014.
- Hewitt, I. J.: Seasonal changes in ice sheet motion due to melt water lubrication, *Earth Planet. Sc. Lett.*, 371–372, 16–25, 2013.
- Hoffman, M. J. and Price, S.: Feedbacks between coupled subglacial hydrology and glacier dynamics, *J. Geophys. Res.-Earth*, 119, 414–436, 2014.
- Hoffman, M. J., Catania, G. A., Neumann, T. A., Andrews, L. C., and Rumrill, J. A.: Links between acceleration, melting, and supraglacial lake drainage of the western Greenland Ice Sheet, *J. Geophys. Res.-Earth*, 116, F04035, doi:10.1029/2010JF001934, 2011.
- IPCC: Climate Change 2007: The Physical Science Basis, in: Contribution of Working Group I to the Fourth Assessment Report of the Intergovernmental Panel on Climate Change, edited by: Solomon, S., Qin, D., Manning, M., Chen, Z., Marquis, M., Averyt, K. B., Tignor, M., and Miller, H. L., Cambridge University Press, Cambridge, UK, 2007.
- Joughin, I., Smith, B. E., Howat, I. M., Scambos, T., and Moon, T.: Greenland flow variability from ice-sheet-wide velocity mapping, *J. Glaciol.*, 56, 415–430, 2010.
- Leeson, A. A., Shepherd, A., Palmer, S., Sundal, A., and Fettweis, X.: Simulating the growth of supraglacial lakes at the western margin of the Greenland ice sheet, *The Cryosphere*, 6, 1077–1086, doi:10.5194/tc-6-1077-2012, 2012.
- Lefebvre, F., Gallée, H., Van Ypersele, J., and Huybrechts, P.: Modelling of large-scale melt parameters with a regional climate model in south Greenland during the 1991 melt season, *Ann. Glaciol.*, 35, 391–397, 2002.
- McMillan, M., Nienow, P., Shepherd, A., Benham, T., and Sole, A.: Seasonal evolution of supra-glacial lakes on the Greenland Ice Sheet, *Earth Planet. Sc. Lett.*, 262, 484–492, 2007.
- Meierbachtol, T., Harper, J., and Humphrey, N.: Basal drainage system response to increasing surface melt on the Greenland ice sheet, *Science*, 341, 777–779, 2013.
- Morriss, B. F., Hawley, R. L., Chipman, J. W., Andrews, L. C., Catania, G. A., Hoffman, M. J., Lüthi, M. P., and Neumann, T. A.: A ten-year record of supraglacial lake evolution and rapid drainage in West Greenland using an automated processing algorithm for multispectral imagery, *The Cryosphere*, 7, 1869–1877, doi:10.5194/tc-7-1869-2013, 2013.
- Nye, J. F.: The distribution of stress and velocity in glaciers and ice sheets, *P. Roy. Soc. Lond. A*, 239, 113–133, 1957.
- Palmer, S., Shepherd, A., Nienow, P., and Joughin, I.: Seasonal speedup of the Greenland Ice Sheet linked to routing of surface meltwater, *Earth Planet. Sc. Lett.*, 302, 423–428, 2011.
- Phillips, T., Rajaram, H., and Steffen, K.: Cryo-hydrologic warming: A potential mechanism for rapid thermal response of ice sheets, *Geophys. Res. Lett.*, 37, L20503, doi:10.1029/2010GL044397, 2010.
- Reeh, N.: Parameterization of melt rate and surface temperature on the Greenland ice sheet, *Polarforschung*, 59, 113–128, 1991.
- Rist, M. A., Sammonds, P. R., Murrell, S. A. F., Meredith, P. G., Doake, C. S. M., Oerter, H., and Matsuki, K.: Experimental and theoretical fracture mechanics applied to Antarctic ice fracture and surface crevassing, *J. Geophys. Res.*, 104, 2973–2986, 1999.
- Schoof, C.: Ice sheet acceleration driven by melt supply variability, *Nature*, 468, 803–806, 2010.
- Schuler, T. V., Loe, E., Taurisano, A., Eiken, T., Hagen, J. O., and Kohler, J.: Calibrating a surface mass-balance model for Austfonna ice cap, Svalbard, *Ann. Glaciol.*, 46, 241–248, 2007.
- Schwanghart, W. and Kuhn, N. J.: TopoToolbox: A set of Matlab functions for topographic analysis, *Environ. Modell. Softw.*, 25, 770–781, 2010.
- Schwanghart, W. and Scherler, D.: Short Communication: TopoToolbox 2 – MATLAB-based software for topographic analysis and modeling in Earth surface sciences, *Earth Surf. Dynam.*, 2, 1–7, doi:10.5194/esurf-2-1-2014, 2014.
- Selmes, N., Murray, T., and James, T. D.: Fast draining lakes on the Greenland Ice Sheet, *Geophys. Res. Lett.*, 38, L15501, doi:10.1029/2011GL047872, 2011.
- Shannon, S. R., Payne, A. J., Bartholomew, I. D., van den Broeke, M. R., Edwards, T. L., Fettweis, X., Gagliardini, O., Gillet-Chaulet, F., Goelzer, H., Hoffman, M. J., Huybrechts, P., Mair, D. W. F., Nienow, P. W., Perego, M., Price, S. F., Smeets, C. J. P. P., Sole, A. J., van de Wal, R. S. W., and Zwinger, T.: Enhanced basal lubrication and the contribution of the Greenland ice sheet to future sea-level rise, *P. Natl. Acad. Sci. USA*, 110, 14156–14161, doi:10.1073/pnas.1212647110, 2013.
- Sole, A., Nienow, P., Bartholomew, I., Mair, D., Cowton, T., Tedstone, A., and King, M. A.: Winter motion mediates dynamic response of the Greenland Ice Sheet to warmer summers, *Geophys. Res. Lett.*, 40, 3940–3944, 2013.
- Sundal, A. V., Shepherd, A., Nienow, P., Hanna, E., Palmer, S., and Huybrechts, P.: Evolution of supra-glacial lakes across the Greenland Ice Sheet, *Remote Sens. Environ.*, 113, 2164–2171, 2009.
- Tedesco, M., Willis, I. C., Hoffman, M. J., Banwell, A. F., Alexander, P., and Arnold, N. S.: Ice dynamic response to two modes of surface lake drainage on the Greenland ice sheet, *Environ. Res. Lett.*, 8, 034007, doi:10.1088/1748-9326/8/3/034007, 2013.
- Tedstone, A. J., Nienow, P. W., Bartholomew, I. D., Sole, A. J., Cowton, T. R., Mair, D. W. F., and King, M. A.: Greenland ice sheet motion insensitive to exceptional meltwater forcing, *P. Natl. Acad. Sci. USA*, 110, 19719–19724, 2013.
- van der Veen, C. J.: Fracture propagation as means of rapidly transferring surface meltwater to the base of glaciers, *Geophys. Res. Lett.*, 34, L01501, doi:10.1029/2006GL028385, 2007.
- Vaughan, D. G.: Relating the occurrence of crevasses to surface strain rates, *J. Glaciol.*, 39, 255–266, 1993.
- Vieli, A., Payne, A. J., Du, Z., and Shepherd, A.: Numerical modelling and data assimilation of the Larsen B ice shelf, Antarctic Peninsula, *Philos. T. Roy. Soc. A*, 364, 1815–1839, 2006.
- Zwally, J. H., Abdalati, W., Herring, T., Larson, K., Saba, J., and Steffen, K.: Surface Melt-Induced Acceleration of Greenland Ice Sheet Flow, *Science*, 297, 218–222, 2002.